Study on fire risk associated with a failure of large-scale commercial $LiFePO_4$/graphite and $LiNi_xCo_yMn_{1-x-y}O_2$/graphite batteries

Authors: Z. Wang, K, Zhu, J. Hu and J. Wang

Journal: *Energy Science and Engineering*

Date: accepted 14 January 2019

Citation: Volume 7, 411 – 419
DOI: 10.1002/ese3.283

Open Access article, PDF attached.

Received: 21 November 2018 | Revised: 24 December 2018 | Accepted: 14 January 2019

DOI: 10.1002/ese3.283

RESEARCH ARTICLE

Energy Science & Engineering Open Access

Study on the fire risk associated with a failure of large-scale commercial $LiFePO_4$/graphite and $LiNi_xCo_yMn_{1-x-y}O_2$/graphite batteries

Zhi Wang[1] | **Kang Zhu**[2] | **Jianyao Hu**[3] | **Jian Wang**[1]

[1]State Key Laboratory of Fire Science, University of Science and Technology of China, Hefei, China

[2]China Aviation Lithium Battery (Jiangsu) Co., Ltd., Changzhou, China

[3]China CEPREI Laboratory, Guangzhou, China

Correspondence
Jian Wang, State Key Laboratory of Fire Science, University of Science and Technology of China, Hefei, China.
Email: wangj@ustc.edu.cn

Funding information
National Key R&D Program of China, Grant/Award Number: 2018YFC0809500; Changzhou Sci&Tech Program, Grant/Award Number: CE20185001; Open Project Program of the State Key Laboratory of Fire Science, Grant/Award Number: HZ2015-KF13

Abstract

The fire hazards of fully charged large-scale commercial $LiFePO_4$/graphite and $LiNi_xCo_yMn_{1-x-y}O_2$/graphite batteries are experimentally studied using a bench-scale calorimetry apparatus. The battery burning process can be roughly summarized into three stages with significant criteria. The fire behaviors associated with $LiNi_xCo_yMn_{1-x-y}O_2$/graphite battery give more splash spark, explosion, and gas/smoke ejection, while $LiFePO_4$/graphite battery presents more jet flame. The sound signal may be a good choice for reflecting the battery state during thermal failure. The battery catches fire when average surface temperature (ST) reaches about 150°C. The maximum average STs for $LiFePO_4$/graphite and $LiNi_xCo_yMn_{1-x-y}O_2$/graphite batteries are approximately 535.3 and 658.7°C, respectively. The maximum heat release rate (HRR) of two batteries is comparable, while the total heat release for $LiFePO_4$/graphite battery is higher than $LiNi_xCo_yMn_{1-x-y}O_2$/graphite battery. The normalized heat release by initial mass of battery is found to be 2.304 and 3.133 kJ/g for $LiFePO_4$/graphite and $LiNi_xCo_yMn_{1-x-y}O_2$/graphite batteries, respectively. Besides, $LiNi_xCo_yMn_{1-x-y}O_2$/graphite battery releases more CO and exhibits larger mass loss compared with $LiFePO_4$/graphite battery. Finally, fire risk assessment for two batteries is also performed and discussed. In conclusion, $LiNi_xCo_yMn_{1-x-y}O_2$/graphite battery is more hazardous than $LiFePO_4$/graphite battery in current condition.

KEYWORDS

battery scheme, fire hazard, gas emissions, heat release

1 | INTRODUCTION

Increasing concerns associated with the energy utilization and environment protection motivate the need of sustainable energy sources, which promotes the development of reliable energy storage systems and devices.[1-3] Lithium ion batteries (LIBs) are now recognized as a better choice in energy storage field and have been widely used in the electronic products such as laptop, mobile cell, digital camera, etc.[4] Recently, LIBs are extended to electric vehicle, wind/solar energy storage, communication backup power, etc.[5,6] Although LIBs exhibit high energy density, low self-discharge, high working voltage, excellent cycle performance, no memory effect, the performance, especially safety performance is gradually becoming a prominent problem.[7] The safety problems for LIBs involving fire or explosion may cause catastrophic consequences. Some accidents related to the thermal hazards of LIBs have been extensively reported.[7,8]

Previous researches on thermal behavior and fire hazards of LIB have been performed at small format battery.[9-17] Factors including the battery materials,[18,19] states of charge (SOC),[20,21] battery states,[22] heating modes,[23] ambient pressures,[13] battery modules,[24] and incident heat fluxes,[8] impacting the fire behavior of LIBs were focused. Ribiere et al[25] identified and quantified the toxic emissions (NO, HCl, HF, etc.) and energy release of small commercial pouch cells by using the Fire Propagation Apparatus. They found that the fully charged battery gave a slightly low total heat release while a relatively high toxic gas emissions. Ditch et al[26] conducted the free-burn fire tests to evaluate the flammability characteristics of cartoned small-format LIBs in warehouse scenarios. Larsson et al[27] exposed the commercial lithium iron phosphate cells and laptop battery packs to a controlled propane fire. They found that battery with higher SOC presented higher heat release rate (HRR) peak and a lower total emission of HF. Chen et al[19] employed a fire calorimeter to investigate the combustion behavior of two commercial 18 650 LIBs at different SOCs. They reported that the HRR and total heat release increased with SOC, and $LiCoO_2$ 18 650 LIB gave higher explosion risk than $LiFePO_4$ 18 650 LIB. A Copper Slug Battery Calorimetry (CSBC) was used by Liu et al[28] to measure the total energy generated inside the battery of 18 650 LIB at various SOCs. Combined with a cone calorimeter, it could quantify the flaming combustion of materials ejected from battery. Liu et al[18] employed the similar experimental technique to measure the heat release of 18 650 LIBs with three different cathodes: lithium cobalt oxide (LCO), lithium nickel manganese cobalt oxide (NMC), and lithium iron phosphate (LFP). The results illustrated that the combustion heat released of 100% SOC LCO and LFP LIBs was comparable, while fully charged NMC LIB released notably large amounts heat. Lyon et al[29] employed a bomb calorimeter to explore energy released by failure of 18 650 LIBs with four different commercial cathode chemistries. Fu et al[8] studied the burning behaviors of 18 650 LIBs under different SOCs and incident heat fluxes using a cone calorimeter. Said et al[2] tested the multiple thermal hazards associated with a failure of prismatic LiCoO2/graphite LIBs. The rate of heat generated inside LIB and the combustion of ejected battery materials were measured and discussed. For large-scale battery, Ping et al,[30] Wang et al[31] and Huang et al[32] investigated the combustion behavior of 50 Ah $LiFePO_4$/graphite and $Li(Ni_xCo_yMn_z)O_2$/LTO batteries by using ISO 9705 combustion room, respectively. However, limited work focuses on the fire risk of large-scale commercial LIBs, especially the comparison among the different battery composition schemes. It is also of a great interest at present. The $LiFePO_4$/graphite and $LiNi_xCo_yMn_{1-x-y}O_2$/graphite batteries commonly used in vehicle and energy storage batteries field are chosen in current work.

In this work, the large-scale commercial fully charged $LiFePO_4$/graphite and $LiNi_xCo_yMn_{1-x-y}O_2$/graphite batteries were used to explore the burning behaviors and fire risk. To characterize the fire risk of LIBs, the main parameters including sound signal, temperature, heat release, gas emissions, and mass loss were measured. The fire hazards corresponding to two composition schemes batteries were also compared and discussed further. The findings may be extend to the battery modules composed of different types of small format batteries, and the larger size batteries to some extent.

2 | EXPERIMENTAL SETUP

Two kinds of large-scale commercial batteries tested in this work are manufactured by China Aviation Lithium Battery Co., Ltd., which are applied to energy storage devices. The

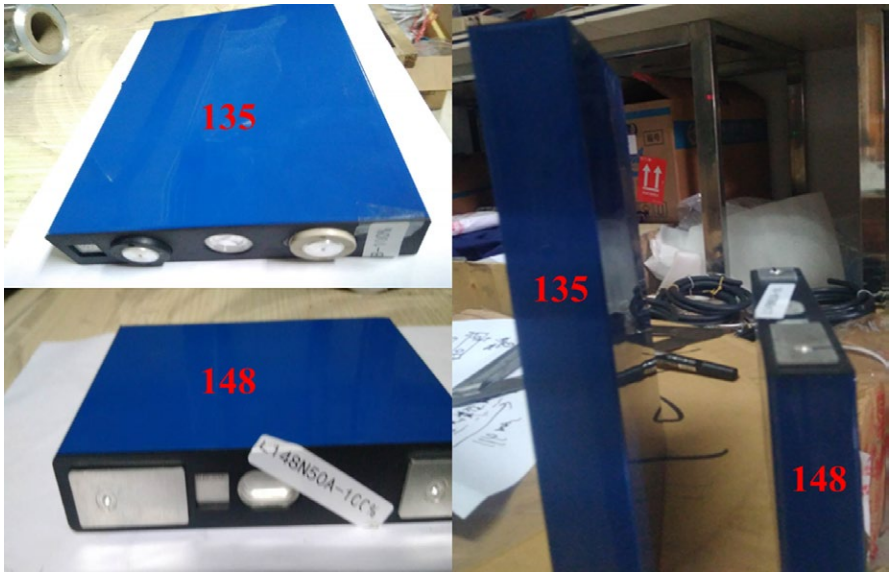

FIGURE 1 Photos of two lithium ion battery samples

photos of LIBS are shown in Figure 1. One of them is LIB with 36.2 wt % $LiFePO_4$ (LFP) as the cathode. The other one is LIB with 36.6 wt % $LiNi_xCo_yMn_{1-x-y}O_2$ (NMC) as the cathode. And the anode of two LIBs is natural graphite about 20 wt %. The electrolyte is the solution of $LiPF_6$ and the mixture of ethylene carbonate (EC), accounting for 23 wt %. The polyethylene (PE) is chosen as the separator approximately 4 wt %. Others including the Al, Cu, polyvinylidene fluoride (PVDF), etc. are about 16.2 wt %. Table 1 presents the detailed information of LIBs. The LIB is charged to the expected SOC and then is allowed to a rest for 24 h prior to all tests.

Figure 2 presents a schematic diagram of the thermal hazard test apparatus. The apparatus was developed to fill the needs of battery thermal runaway and burning test based on the full scale room test (ISO 9705) and the cone calorimeter test (ISO 5660). The battery sample was placed and installed horizontally on a sample holder made by stainless mesh. An electrical balance was applied to record the mass loss of sample. The K-type thermocouples with diameter of 1 mm were attached on the surface of battery to measure the surface temperature (ST) profiles. The gaseous products of combustion were collected and analyzed by a Servomex 4100 gas analyzer (Servomex, East Sussex, UK), which would be devoted to measuring the concentrations of CO_2, CO and O_2, and estimating the HRR based on the oxygen depletion method. An electric heater with a power of 2 kW was taken as an external heating source to heat the battery and trigger the thermal runaway of battery. A digital camera with a high resolution of 25 fps was used to record the whole experimental process for obtaining the visually visible photographs.

3 | RESULTS

3.1 | General observations

Figure 3 shows the typical sequence photos of the experiment. The significant thermal behaviors both 135 LIB and 148 LIB can be clearly seen. The whole process can be roughly divided into three stages: stage (a)-LIB is heated to ignite, stage (b)-LIB is involved in splash spark, hissing sound, jet flame, general flame, explosion and gas/smoke ejection, and stage (c)-LIB is gradually out of flame. Multiple outbursts from the battery are visually observed. However, the difference of the composition between the 135 LIB and 148 LIB may cause completely different burning behaviors. Apparently, 135 LIB presents more vigorous bright flame, while 148 LIB exhibits more violent explosion and gas emission. In addition, the time to ignition (TTI) of 135 LIB and 148 LIB is approximately of 525.4 and 368.2 seconds, respectively. The duration of combustion process is about 443.5 and 156.1 seconds for 135 LIB and 148 LIB, respectively. All the above indicates that 148 LIB is easier to ignite and burns faster than 135 LIB, which reflects that the thermal stability of 148 LIB is less than that of 135 LIB to some extent. Figure 4 depicts the original sound recorded in the whole experimental process. The data can also reflect the fierce level of combustion and the different thermal stages. This may provide

TABLE 1 Information of batteries tested in this study

Sample	Cathode	Length, mm	Width, mm	Height, mm	Normal capacity, Ah	Weight, g	SOC, %
135	LFP	135.2	29.5	220.5	80	1826.9	100
148	NMC	148.3	26.7	98.0	50	909.8	100

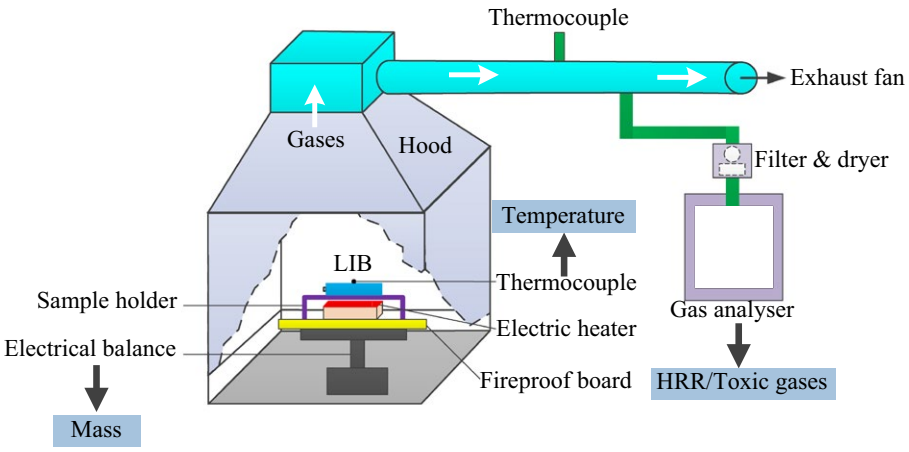

FIGURE 2 Schematic illustration of the experimental setup

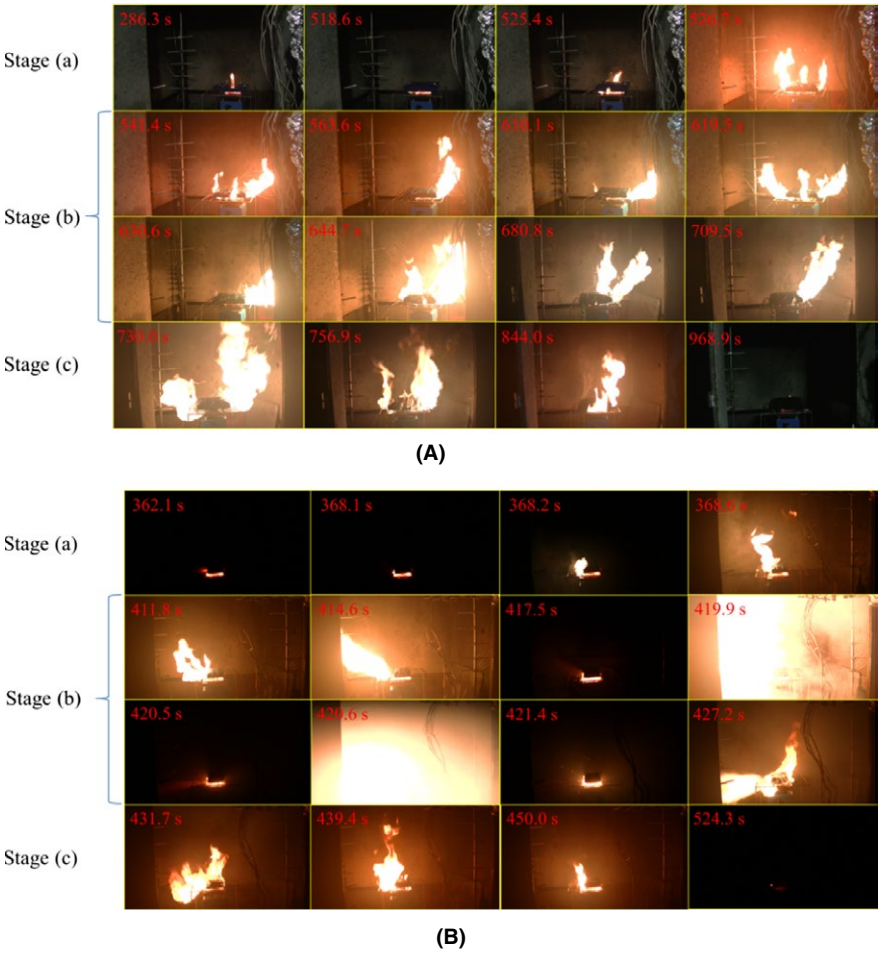

FIGURE 3 The representative phenomenon over time in the experiment. A, 135 LIB; B, 148 LIB

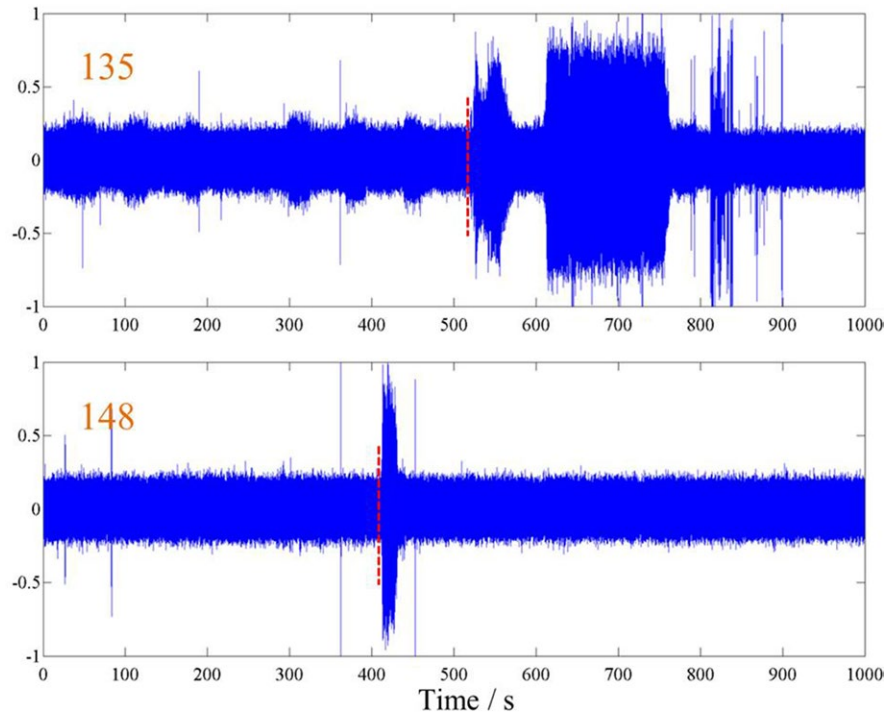

FIGURE 4 The original sound in the process of experiment

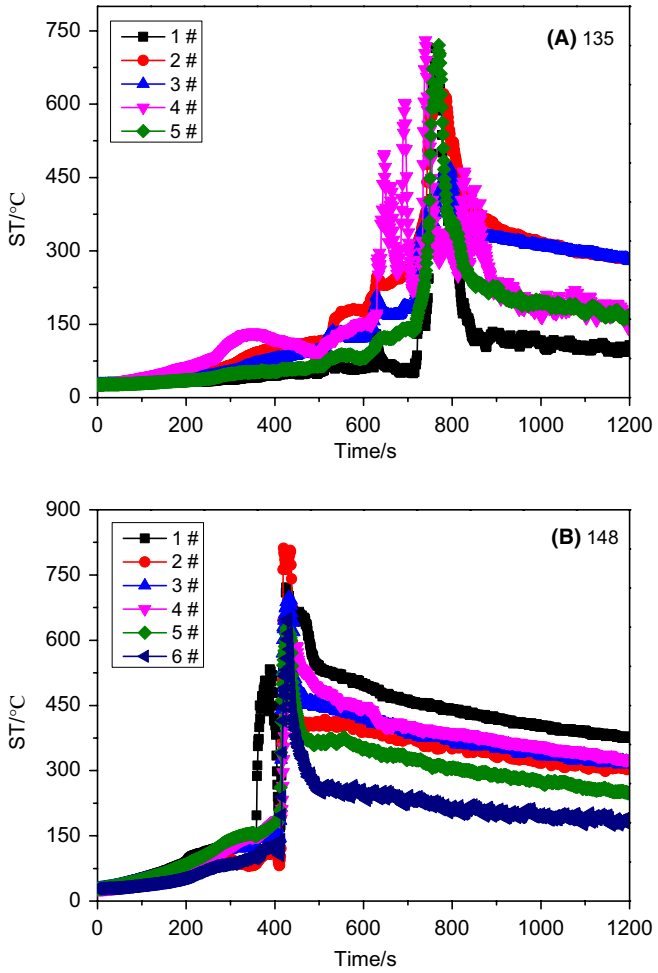

FIGURE 5 Surface temperature curves of the lithium ion battery. A, 135; B, 148

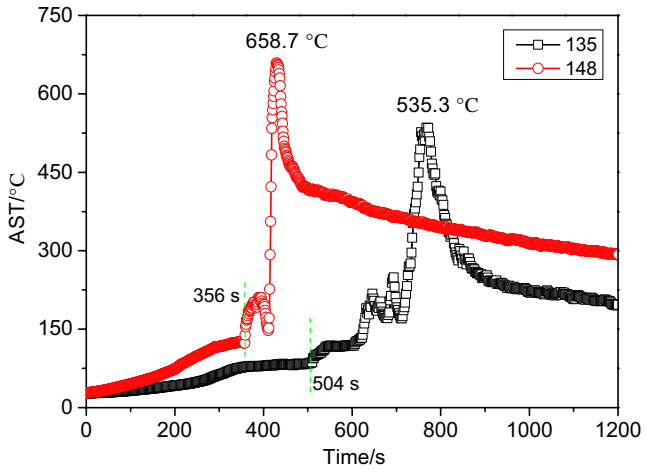

FIGURE 6 The average surface temperature of the lithium ion battery

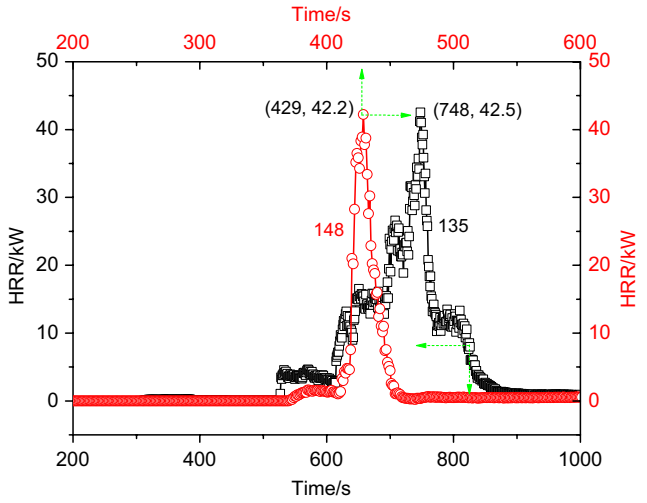

FIGURE 7 Heat release rate of the lithium ion battery

guidance for the fire detection and rescue of LIB based on a new perspective.

3.2 | Surface temperature

The ST is a key parameter reflecting the thermal failure of LIB. Considering the nonuniform temperature distribution of large-scale battery, six thermocouples are used to monitor the ST. The temperature profiles of LIB are shown in Figure 5. For 135 LIB, the 6 # thermocouple detects no temperature data due to the shedding of itself. It should be noticed that the ST has a slight variation at different points for both 135 LIB and 148 LIB. However, there is an observed difference of the temperature profile for 135 LIB and 148 LIB. Finally, the average ST (AST) is calculated to represent the ST. Figure 6 describes the average ST of the LIB. It can be found that the thermal runaway of 135 LIB is at 504 seconds and 148 LIB is at 356 seconds. The maximum AST is 535.3 and 658.7°C for 135 LIB and 148 LIB, respectively. The 148 LIB has a higher temperature increasing rate than the 135 LIB. The maximum increasing rates of 135 LIB and 148 LIB are about 18.04 and 64.84°C/s, respectively. It is confirmed that the 148 LIB gives a more thermally reactive response.

3.3 | Heat release and gas emissions

The heat release rate results for 135 LIB and 148 LIB are illustrated in Figure 7. In current work, the HRR estimated is based on the oxygen consumption, corrected by carbon dioxide and carbon monoxide production. The HRR curve is not smooth like general combustibles and presents several transition phases. This coincides with the complex thermally reactive behaviors of LIB. The calculation results show that the maximum HRR value reaches approximately 42.5 kW at 429 seconds and 42.2 kW at 748 seconds for 135 LIB and 148 LIB, respectively. Besides, the HRR profile is integrated with time to allow the evaluation of the

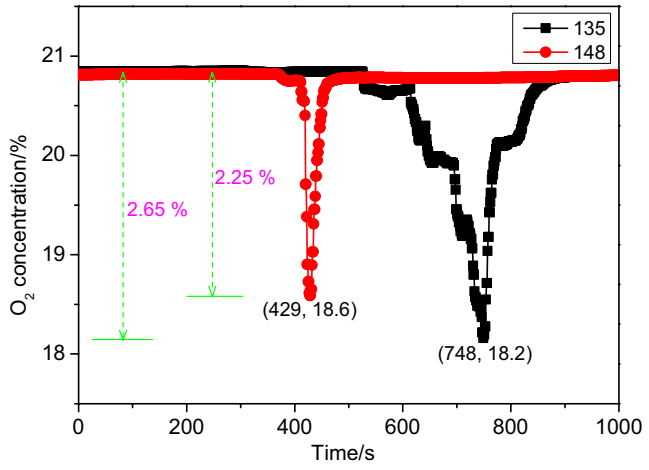

FIGURE 8 Oxygen consumption in the experiment

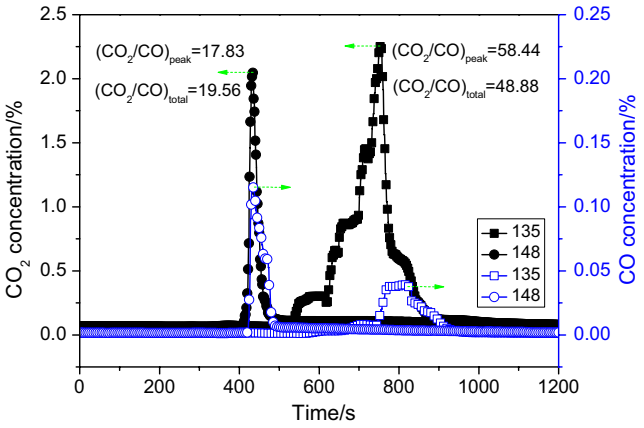

FIGURE 9 Gas emission in the experiment

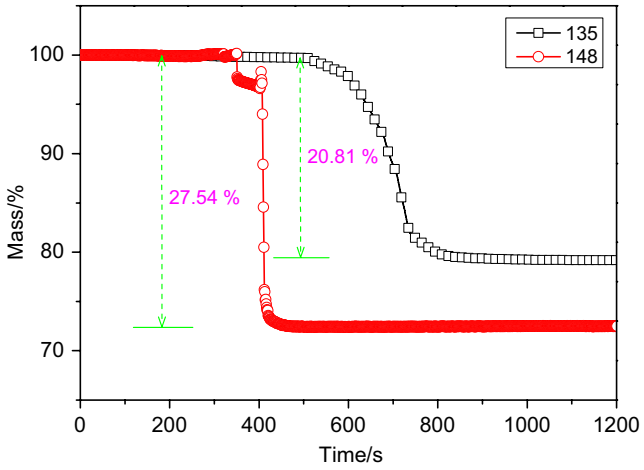

FIGURE 10 Mass loss of the lithium ion battery

total heat release. The calculated values are 4209 kJ and 865 kJ for 135 LIB and 148 LIB, respectively. Note that 148 LIB discloses a higher reaction rate and the combustion heat released shortly causes an explosion risk, which is consist with the above thermal behavior and temperature analysis.

Another critical factor related to battery combustion is the gases depletion and emission. During the whole experimental process, the O_2 is consumed and the CO and CO_2 are emitted. The gas concentrations and emission yields are continuously measured by a Servomex 4100 gas analyzer. The gas analysis from the battery combustion allows assessing the heat release, combustion efficiency, and toxic threat. Figure 8 shows the evaluation of O_2 consumption. The maximum consumption value of oxygen is about 2.65% and 2.25% for 135 LIB and 148 LIB, respectively. Figure 9 illustrates the concentration of gaseous emissions. It can be noted that the content of CO_2 is significant higher than CO, regardless of the battery formats. The ratios of peak and total contents between CO_2 and CO are 58.44 and 48.88 for 135 LIB, while they are 17.83 and 19.56 for 148 LIB. This result highlights that the 135 LIB has higher combustion efficiency and lower toxic risk.

3.4 | Mass loss

The mass loss of battery is measured by using a Mettler Toledo XP10002S with a range of 0-9 kg and a readability of 0.01 g. The battery mass at different times is normalized by the original mass. 20.81% mass loss of 135 LIB is obtained and the data are about 27.54% for 148 LIB. The maximum mass loss rate is also estimated. They are 0.25% s^{-1} and 4.71% s^{-1} for 135 LIB and 148 LIB, respectively. Note that 148 LIB reveals a larger and faster mass loss, which indicates that the 148 LIB may exhibit violent chemical reactions and incomplete combustion combining the analysis of heat release and gas emission (Figure 10).

4 | DISCUSSION

In the process of thermal analysis of LIB, it was always be simplified as an isotropy and homogenous structure. For a prismatic LIB in current work, the bottom surface of battery was heated by an electric heater, and the top and lateral surfaces were exposed to the ambient atmosphere. The thermal balance of battery can be dominated by heat accumulation and heat loss, as expressed in the following conversation equation:[5]

$$\frac{\partial\left(\rho C_p T\right)}{\partial t}=\dot{Q}_{\text{input}}+\dot{Q}_{\text{chem}}-\dot{Q}_{\text{loss}}, \tag{1}$$

where ρ C_p and T are the density, the specific heat and the temperature, respectively, t is the time, $\dot{Q}_{\text{input}}$, $\dot{Q}_{\text{chem}}$ and $\dot{Q}_{\text{loss}}$ are the input heat of the external heater, the heat generation by the chemical reaction, and the heat loss from battery, respectively.

As the battery temperature increasing, several superheated side reactions including the decomposition of solid

TABLE 2 Comparison of main parameters related to the fire hazards of the lithium ion batteries (LIBs)

LIB	135	148
Maximum AST, °C	535.3	658.7
Maximum AST increasing rate, °C/s	18.04	64.84
Time to ignition, s	**525**	**368**
Time to peak HRR, s	748	429
Peak HRR, kW	42.5	42.2
Normalized peak HRR, kW/m^2	1426.2	2910.3
Normalized by initial mass, kW/g	**0.023**	**0.046**
Combustion time, s	444	156
Total heat release, MJ	4.21	2.85
Normalized total heat release, MJ/m^2	141.2	195.8
Normalized by initial mass, kJ/g	**2.304**	**3.133**
Peak CO_2 concentration, %	2.25	2.05
Peak CO concentration, %	0.0385	0.1150
Total mass loss, g	**380.2**	**250.6**
Maximum mass loss rate, %/s	0.25	4.71
***X* parameter, kW/m^2/s**	**2.72**	**7.91**

The bold values represent the key parameter

electrolyte interface (SEI) film, cathode materials decomposing, electrolyte decomposing, the reaction between the binder and the high activity anode, etc. inside the battery would produce heat which can be described as follows:[3]

$$\dot{Q}_{\text{chem}} = \Delta H M^n A \exp\left(-\frac{E_a}{RT}\right), \tag{2}$$

where ΔH, M and R are the reaction heat, the mass of reactants and the gas constant, respectively, n, A and E_a are the reaction order, the pre-exponential factor, and the activation energy, respectively. The decomposition temperature of SEI is about 80-120°C. As the temperature increases to 110°C, some combustible gases will be released due to electrolyte decomposition. With a continuous increase of temperature, the separator will melt at 135-160°C, and the cathode will decompose above 200°C. Finally, the battery becomes unstable and is out of control.

The 135 LIB with LFP as cathode has good thermal stability than the 148 LIB employed NMC as cathode. Compared with the NMC, the LFP shows excellent thermal tolerance against $LiPF_6$-based electrolyte, which can suppress the decomposition of electrolyte and has a slight structure change to some extent.[33] It may be reflected in the earlier and easier thermal failure for 148 LIB than that for 135 LIB. However, NMC underwent a phase transition from layered structure to crystalline structure with a space group Fm3m in the range of 220-350°C.[34] The overall decomposition reaction of NMC can be expressed as:[15]

$$\text{NMC}\left(R_3 - m\right) \overset{\Delta T,\text{solv.}}{\rightarrow} (\text{Mn, Ni})\,\text{O}\,(\text{Fm3m}) + \text{CoO} + \text{Ni} + \text{O}_2. \tag{3}$$

Thus, it should be noted that the oxygen was released. Similarly, the oxygen generated from the LFP cathode can also described as:

$$4\text{FePO}_4 \rightarrow 2\text{Fe}_2\text{P}_2\text{O}_7 + \text{O}_2. \tag{4}$$

Following, the released oxygen would react with EC, as shown in the reaction:

$$\text{C}_3\text{H}_4\text{O}_3 + \frac{5}{2}\text{O}_2 \rightarrow 3\text{CO}_2 + 2\text{H}_2\text{O}. \tag{5}$$

Based on these analyses, it can be conjectured that the thermal hazard of LIB was induced by the large amount of heat accumulation and gases generation caused by the chemical reactions involving the cathode, electrolyte, and dropped electrode materials. The 135 LIB released combustible gases, accompanied by inner pressure decreasing and immediately followed by a considerable jet fire. In addition to fire and explosion, the 148 LIB experienced multiple gas/smoke ejections without flame. However, the emitted flammable and toxic gases can be a serious problem for LIB fire. Swelling was also observed for two formats battery. Finally, the distinguishing thermal behaviors can be explained by the different thermal failure mechanisms of two composition batteries attributed to the varied type and intensity chemical reactions. That is deserved to have an in-depth study in future work.

Table 2 shows the comparison of parameters associated with fire hazards of the LIBs. It can be seen that the composition scheme of battery is a key factor for fire risk of battery. Compare to 135 LIB, the 148 LIB is the most hazardous and illustrates a potential threat for the safety based on an evaluation method proposed by Petrella.[35] Besides, the toxic risk is also obvious for 148 LIB according to the production of CO and CO_2. In summary, 148 LIB has a higher overall reactivity and fire hazard than 135 LIB in current study.

5 | CONCLUSIONS

In this work, the fire hazard associated with the failure of large-scale battery was examined experimentally under fully charged. Two commercial composition schemes of LIB commonly applied in electric vehicles were selected to facilitate the study. One is $LiFePO_4$/graphite battery (135 LIB). The other is $LiNi_xCo_yMn_{1-x-y}O_2$/graphite battery (148 LIB). The thermal behavior, sound signal, ST, heat release, gas emission, and mass loss were recorded and measured. The effect of composition scheme on fire hazard of battery was also discussed.

The whole experimental process can be roughly divided into three representative phases, regardless of 135 LIB and 148 LIB. However, 148 LIB presents more splash spark, explosion, and gas/smoke ejection in stage (b) while the jet flame is the main thermal behavior for 135 LIB. The sound signal can also reflect the battery failure state during the experiments. Besides, it is illustrated that the thermal failure and ignition of 148 LIB are relatively easier than that of 135 LIB. Compared with 135 LIB, 148 LIB combusts incompletely, taking the consumption of O_2, the generation of CO_2 and CO, and the mass loss of battery into account. But, the normalized heat release by initial mass of battery was calculated. The value obtained as 2.304 kJ/g for 135 LIB is less than 3.133 kJ/g for 148 LIB, which is significantly lower than that of commonly solid combustibles. Meanwhile, 148 LIB releases approximately 3.0 times more toxic CO than 135 LIB. The total mass loss is about 380.2 and 250.6 g for 135 LIB and 148 LIB, respectively. Finally, we conducted the systematic assessment of fire risk for batteries and the fire risk of two batteries was evaluated by Petrella method. In summary, 148 LIB is more hazardous than 135 LIB based on normalized heat release and toxic gas emissions in current work. Certainly, the active components inside battery mainly determine the fire behavior of integral battery. Thus, the fire performance of each active component will be further checked and the comprehensive comparative study will be fulfilled in the future work.

ACKNOWLEDGMENTS

This work was supported by the National Key R&D Program of China (No. 2018YFC0809500), the Changzhou Sci&Tech Program (No. CE20185001), the Open Project Program of the State Key Laboratory of Fire Science (No. HZ2015-KF13). The authors would also like to express their great gratitude to the reviewers for their valuable comments and suggestions.

ORCID

Jian Wang [redacted]

REFERENCES

1. Poizot P, Dolhem F. Clean energy new deal for a sustainable world: from non-CO_2 generating energy sources to greener electrochemical storage devices. *Energy Environ Sci*. 2011;4(6):2003-2019.
2. Said AO, Lee C, Liu X, Wu Z, Stoliarov SI. Simultaneous measurement of multiple thermal hazards associated with a failure of prismatic lithium ion battery. *Proc Combust Inst*. 2018. https://doi.org/10.1016/j.proci.2018.05.066
3. Wang Q, Ping P, Zhao X, Chu G, Sun J, Chen C. Thermal runaway caused fire and explosion of lithium ion battery. *J Power Sources*. 2012;208:210-224.
4. Balakrishnan PG, Ramesh R, Kumar TP. Safety mechanisms in lithium-ion batteries. *J Power Sources*. 2006;155(2):401-414.
5. Liu J, Wang Z, Gong J, Liu K, Wang H, Guo L. Experimental study of thermal runaway process of 18650 lithium-ion battery. *Mater*. 2017;10(3):230.
6. Wang J, Yamada Y, Sodeyama K, et al. Fire-extinguishing organic electrolytes for safe batteries. *Nat Energy*. 2018;3(1):22-29.
7. Liu K, Liu Y, Lin D, Pei A, Cui Y. Materials for lithium-ion battery safety. *Sci Adv*. 2018;4(6):eaas9820.
8. Fu Y, Lu S, Li K, Liu C, Cheng X, Zhang H. An experimental study on burning behaviors of 18650 lithium ion batteries using a cone calorimeter. *J Power Sources*. 2015;273:216-222.
9. Yim T, Park MS, Woo SG, et al. Self-extinguishing lithium ion batteries based on internally embedded fire-extinguishing microcapsules with temperature-responsiveness. *Nano Lett*. 2015;15(8):5059-5067.
10. Andersson P, Blomqvist P, Lorén A, Larsson F. Using Fourier transform infrared spectroscopy to determine toxic gases in fires with lithium-ion batteries. *Fire Mater*. 2016;40(8):999-1015.
11. Chen M, Liu J, Lin X, Huang Q, Yuen R, Wang J. Combustion characteristics of primary lithium battery at two altitudes. *J Therm Anal Calor*. 2016;124(2):865-870.
12. Chung YH, Jhang WC, Chen WC, Wang YW, Shu CM. Thermal hazard assessment for three C rates for a Li-polymer battery by using vent sizing package 2. *J Therm Anal Calor*. 2017;127(1):809-817.
13. Chen M, Liu J, He Y, Yuen R, Wang J. Study of the fire hazards of lithium-ion batteries at different pressures. *Appl Therm Eng*. 2017;125:1061-1074.
14. Walters RN, Lyon RE, eds. Energy release from lithium ion batteries in the bomb calorimeter. 14th International Conference and Exhibition on Fire and Materials 2015; 2015: Interscience Communications Ltd.
15. Zhong G, Mao B, Wang C, et al. Thermal runaway and fire behavior investigation of lithium ion batteries using modified cone calorimeter. *J Therm Anal Calor*. 2018. https://doi.org/10.1007/s10973-018-7599-7
16. Jiang F, Liu K, Wang Z, Tong X, Guo L. Theoretical analysis of lithium - ion battery failure characteristics under different states of charge. *Fire Mater*. 2018;42:680-686.
17. Fu Y, Lu S, Shi L, Cheng X, Zhang H. Ignition and combustion characteristics of lithium ion batteries under low atmospheric pressure. *Energy*. 2018;161:38-45.
18. Liu X, Wu Z, Stoliarov SI, Denlinger M, Masias A, Snyder K. Heat release during thermally-induced failure of a lithium ion battery: impact of cathode composition. *Fire Saf J*. 2016;85:10-22.
19. Chen M, Zhou D, Chen X, et al. Investigation on the thermal hazards of 18650 lithium ion batteries by fire calorimeter. *J Therm Anal Calor*. 2015;122(2):755-763.
20. Chen M, Dongxu O, Cao S, Liu J, Wang Z, Wang J. Effects of heat treatment and SOC on fire behaviors of lithium-ion batteries pack. *J Therm Anal Calor*. 2018;00:1-9.
21. Chen W-C, Li J-D, Shu C-M, Wang Y-W. Effects of thermal hazard on 18650 lithium-ion battery under different states of charge. *J Therm Anal Calor*. 2015;121(1):525-531.
22. Ouyang D, He Y, Chen M, Liu J, Wang J. Experimental study on the thermal behaviors of lithium-ion batteries under discharge and overcharge conditions. *J Therm Anal Calor*. 2018;132(1):65-75.

23. Wu T, Chen H, Wang Q, Sun J. Comparison analysis on the thermal runaway of lithium-ion battery under two heating modes. *J Hazard Mater*. 2018;344(Supplement C):733-741.
24. Chen M, Yuen R, Wang J. An experimental study about the effect of arrangement on the fire behaviors of lithium-ion batteries. *J Therm Anal Calor*. 2017;129(1):181-188.
25. Ribière P, Grugeon S, Morcrette M, Boyanov S, Laruelle S, Marlair G. Investigation on the fire-induced hazards of Li-ion battery cells by fire calorimetry. *Energy Environ Sci*. 2012;5(1):5271-5280.
26. Ditch B, Yee G, Chaos M, eds. Estimating the time-of-involvement of bulk packed lithium-ion batteries in a warehouse storage fire. 11th International Symposium on Fire Safety Science, FSS 2014; 2014: International Association for Fire Safety Science.
27. Larsson F, Andersson P, Blomqvist P, Lorén A, Mellander BE. Characteristics of lithium-ion batteries during fire tests. *J Power Sources*. 2014;271:414-420.
28. Liu X, Stoliarov SI, Denlinger M, Masias A, Snyder K. Comprehensive calorimetry of the thermally-induced failure of a lithium ion battery. *J Power Sources*. 2015;280:516-525.
29. Lyon RE, Walters RN. Energetics of lithium ion battery failure. *J Hazard Mater*. 2016;318:164-172.
30. Ping P, Wang Q, Huang P, et al. Study of the fire behavior of high-energy lithium-ion batteries with full-scale burning test. *J Power Sources*. 2015;285:80-89.
31. Wang Q, Huang P, Ping P, Du Y, Li K, Sun J. Combustion behavior of lithium iron phosphate battery induced by external heat radiation. *J Loss Prev Process Ind*. 2017;49:961-969.
32. Huang P, Wang Q, Li K, Ping P, Sun J. The combustion behavior of large scale lithium titanate battery. *Sci Rep*. 2015;5:7788. https://doi.org/10.1038/srep07788
33. Yu Y, Wang J, Zhang P, Zhao J. A detailed thermal study of usual LiNi0.5Co0.2Mn0.3O2, LiMn2O4 and LiFePO4 cathode materials for lithium ion batteries. *J Energy Storage*. 2017;12:37-44.
34. Röder P, Baba N, Wiemhöfer H-D. A detailed thermal study of a Li [Ni0. 33Co0. 33Mn0. 33] O2/LiMn2O4-based lithium ion cell by accelerating rate and differential scanning calorimetry. *J Power Sources*. 2014;248:978-987.
35. Petrella RV. The assessment of full-scale fire hazards from cone calorimeter data. *J Fire Sci*. 1994;12(1):14-43.

How to cite this article: Wang Z, Zhu K, Hu J, Wang J. Study on the fire risk associated with a failure of large-scale commercial $LiFePO_4$/graphite and $LiNi_xCo_yMn_{1-x-y}O$ /graphite batteries. *Energy Sci Eng*. 2019;7:411–419.